Applied Catalysis B: Environmental 89 (2009) 510–518

Contents lists available at ScienceDirect

Applied Catalysis B: Environmental

journal homepage: www.elsevier.com/locate/apcatb

# Effect of continuous addition of $H_2O_2$ and air injection on ferrioxalate-assisted solar photo-Fenton degradation of Orange II

J.M. Monteagudo *, A. Durán, I. San Martín, M. Aguirre

*Universidad de Castilla-La Mancha, Departamento de Ingeniería Química, Escuela Técnica Superior de Ingenieros Industriales, Avda. Camilo José Cela, 1, 13071 Ciudad Real, Spain*

ARTICLE INFO

*Article history:*
Received 19 November 2008
Received in revised form 15 January 2009
Accepted 18 January 2009
Available online 24 January 2009

*Keywords:*
Orange II
Ferrioxalate
Photo-Fenton
Neural networks
CPC

ABSTRACT

An experimental study based on ferrioxalate-assisted solar photo-Fenton (SPFox) process shows how non-biodegradable azo dye Orange II (OII) solutions degradation can be enhanced or slowed down by continuous addition of hydrogen peroxide and air injection depending on operation conditions. The decoloration and mineralization of dye solution has been carried out in a solar Compound Parabolic Collector (CPC). An optimization study was done by using Multivariate Experimental Design including the following variables: flow rate of $H_2O_2$, air flow rate, pH and initial concentrations of Fe(II) and oxalic acid. The efficiency of photocatalytic degradation was determined from the analysis of color and Total Organic Carbon (TOC). Experimental data were fitted using neural networks (NNs) which allow the simulation of the process for any value of variables in the studied experimental range. The results reveal that the continuous addition of $H_2O_2$ improves the photocatalytic efficiency since the scavenger effect of peroxide is minimized. On the other hand, this system permits the use of a ferrous concentration below the discharge legal limit (2 ppm) being bubbling of air not necessary in that conditions. In addition, oxalic acid can be used to pH adjustment, reducing the operation costs of Fe removal, chemicals and electric power. Under the optimal conditions, 100% decoloration of dye solution can be reached by using both processes (SPFox with $H_2O_2$ addition at the beginning or along the reaction) but with different reaction rates. However, the efficiency of TOC removal was higher in the SPFox process with continuous addition of $H_2O_2$ (95% TOC removal in SPFox system with continuous addition of peroxide versus 80% TOC removal in SPFox system when peroxide is added at the beginning of the reaction). Molecular and/or radical reaction pathway was studied by conducting the reaction in the presence and absence of *tert*-butylalcohol.



## 1. Introduction

The textile industry produces large quantities of wastewater that contain significant concentrations of contaminants that can be characterized as high levels of total organic content and of color. To avoid the environmental impact generated by the discharge of this type of toxic pollutants, an efficient treatment of these effluents has to be developed.

Thus, the so-called advanced oxidation processes (AOPs) have emerged as water treatment technologies for the mineralization of non-biodegradable aromatics present in dye molecules into $CO_2$, $H_2O$ and inorganic ions [1]. Among AOPs, homogeneus Fenton reaction (system Fe(II)/$H_2O_2$) is one of the most important processes to generate hydroxyl radicals, $^{\bullet}OH$ [2]. Besides, it is well known that when Fenton's reagent is combined with UV–vis irradiation (photo-Fenton system), the efficiency of degradation is considerably improved due to the continuous regeneration of $Fe^{2+}$ via photoreduction of $Fe^{3+}$ and extra generation of new $^{\bullet}OH$ radicals with $H_2O_2$ [3].

However, the production of photons with artificial ultraviolet light sources requires an important electrical energy demand [4] and therefore more environmentally benign and cost-effective methods are desirable. As alternative to UV lamps, solar technology can be successfully used being an economically viable process since solar energy is an abundant natural energy source and can be used instead of artificial light sources which are costly and hazardous [5,6].

On the other hand, $H_2O_2$ has a low molar extinction coefficient, and so it only uses photons that represent minority of total solar radiation, below 350–400 nm, around 3% of solar irradiation [7]. To solve this inconvenience, ferrioxalate can be used since it is a photosensitive complex that is able to expand the usage of solar spectrum range up to 450 nm (≈18% of solar irradiation) improving the oxidation efficiency of the solar photo-Fenton (SPFox) process [8,9]. Besides, ferrioxalate photochemistry provides extra sources of oxidant $H_2O_2$ and catalyst $Fe^{2+}$ for the Fenton

* Corresponding author. Tel.: +34 926 295300; fax: +34 926 295361.
*E-mail address:* josemaria.monteagudo@uclm.es (J.M. Monteagudo).

0926-3373/$ – see front matter © 2009 Published by Elsevier B.V.
doi:10.1016/j.apcatb.2009.01.008

reaction to yield more •OH radicals [10–13] according to the following reactions:

$$[Fe(C_2O_4)_3]^{3-} + h\nu \rightarrow Fe^{2+} + 2C_2O_4^{2-} + C_2O_4^{\bullet-} \quad (1)$$

$$C_2O_4^{\bullet-} + [Fe(C_2O_4)_3]^{3-} \rightarrow Fe^{2+} + 3C_2O_4^{2-} + 2CO_2 \quad (2)$$

$$C_2O_4^{\bullet-} + O_2 \rightarrow 2CO_2 + O_2^{\bullet-} \quad (3)$$

$$O_2^{\bullet-} + H^+ \rightarrow HO_2^{\bullet} \quad (4)$$

$$HO_2^{\bullet} + HO_2^{\bullet} \rightarrow H_2O_2 + O_2 \quad (5)$$

$$H_2O_2 + Fe^{2+} \rightarrow Fe^{3+} + {}^{\bullet}OH + OH^- \quad (6)$$

In recent years, ferrioxalate has been widely used in the photo-Fenton reaction involving ferric compounds, but there is very little information on the ferrioxalate-assisted photo-Fenton systems using ferrous initiated processes. The use of ferrous sulphate is advantageous since it is less corrosive than ferric salts, very cheap and more soluble than ferric compounds. As previously reported [14], the authors studied the degradation of Orange II (OII) solutions appearing in the manufacturing wastewaters of dyeing of textiles, using a ferrioxalate-assisted solar photo-Fenton system with hydrogen peroxide addition at the beginning of the reaction. The obtained results revealed that Fe(II) can significantly accelerate the decomposition of $H_2O_2$ to form more hydroxyl radicals and consequently to increase the degradation efficiency, but the radicals scavenger effect of excess peroxide was detrimental to the photocatalytic process since the catalytic activity was reduced by reaction between •OH radicals and peroxide according to Eq. (7):

$$H_2O_2 + {}^{\bullet}OH \rightarrow HO_2^{\bullet} + H_2O \quad (7)$$

Besides, although other radicals ($HO_2^{\bullet}$) were produced, their oxidation potential is much smaller than that of the hydroxyl radicals. Additionally, according to Eqs. (5), (7) and (8), decomposition of hydrogen peroxide to form water and oxygen was also favoured.

$$ {}^{\bullet}OH + {}^{\bullet}OH \rightarrow H_2O_2 \quad (8)$$

One way to overcome this problem would be to continuously dose $H_2O_2$ along the reaction to minimize the scavenger effect. On the other hand, the iron ions removal from the treated water at the end of the process is costly since it needs a large amount of chemicals and manpower and so it would be advantageous the use of ferrous concentrations below discharge limits. Besides, the production of ferric hydroxide sludge may create other environmental problem [15].

To overcome these drawbacks, in this work, a series of experiments was carried out with $H_2O_2$ added at a constant flow rate into the reactor along the reaction to testing if the hydroxyl radical scavenger effect could be minimized. On the other hand, we have studied the viability of using low iron concentrations (below discharge limit according to the European Union Directive [16]) to avoid the ulterior Fe removal process thus reducing operation costs. Besides, the bubbling of an air stream in the reservoir tank of Compound Parabolic Collector (CPC) reactor all along the reaction time to find out the effect on oxidation reactions and the influence of temperature, pH, and initial oxalic acid concentration were also evaluated.

To determine the optimal values of experimental variables for color removal and mineralization of dye solutions, a Multivariate Experimental Design was performed according to the methodology of response surface [17]. Results of experimental tests were fitted using neural networks (NNs) [18–20], which allows the values of kinetic degradation rate constants (response function) to be estimated within the studied range as a function of process factors. The decrease of color and Total Organic Carbon (TOC) content was monitored.

## 2. Experimental

### 2.1. Materials

Orange II solutions were prepared dissolving Orange II (Aldrich, disodium salt, dye content 85%) in distilled water, without further purification. $FeSO_4{\cdot}7H_2O$ (Panreac, analytical grade) and $H_2C_2O_4{\cdot}2H_2O$ (Panreac, 99.5%) were added to the wastewater to form ferrioxalate complexes to be used in situ immediately because of its light sensitivity. The initial concentration of dye was always 20 ppm.

In all experiments, an initial amount of commercial hydrogen peroxide (30% w/v, Merck) was added to the reactor (≈8 ml) to bring the $H_2O_2$ initial concentration to 75 ppm at the beginning of the reaction after addition of Fe(II) and oxalic acid and pH adjustment. At the same time, the irradiation started, at time $t = 0$, and an air stream was bubbled in the reservoir tank using a compressor (RIETSCHLE) coupled with a COMAQUINSA model R-005 rotameter. Along the reaction, $H_2O_2$ was added through a needle (inner diameter, 3 mm) at a selected flow constant rate (between 0 and 1 ml $min^{-1}$) by means of a precision syringe pump (Terumo, model STC-521) coupled with a 60 ml syringe. The needle extended 70 cm into the reactor with the tip immersed in the liquid. At the end of the experiment, between 45 and 50 ml of peroxide solution has been added to the reactor. The small addition of $H_2O_2$ solution and the periodic removal of solution samples do not significantly change the volume of the reaction mixture (35 L). 0.1 M $H_2SO_4$ and 6 M NaOH solutions were used to pH adjustment of the dye solutions prior to degradation. Before analysis, all the samples were withdrawn from the reactor and immediately treated with excess $Na_2SO_3$ solution to prevent further oxidation.

### 2.2. Irradiation experiments

The decoloration and mineralization of the dye solutions was carried out by using solar light. The experimental setup (Fig. 1) based on a previous study [21] shows the solar reactor (50 L) that consists of a continuously stirred tank, a centrifugal recirculation pump, an solar collector unit with an area of 2 $m^2$ (concentration factor = 1) in an aluminium frame mounted on a fixed south-facing platform tilted 45° in Ciudad Real (Spain) and connecting tubing and valves. This solar unit has 16 borosilicate-glass tubes (OD 32 mm, transmissivity >50% at $\lambda > 300$ nm; >75% at $\lambda > 320$ nm; >90% at $\lambda > 350$ nm) connected by plastic joints, and the total illuminated volume inside the absorber tubes is 16 L. The plant was equipped with a radiometer (model ACADUS 85) tilted 45°, which allowed measuring the received UV-A irradiation (315–400 nm) and provides data in terms of incident solar power, W $m^{-2}$, and accumulated solar energy, W h, by means of a PLC (Programmable Logic Controller) coupled with the radiometer. All photocatalytic experiments were carried out under solar illumination on sunny days of February to June 2008, between 12 a.m. and 4 p.m. For every reaction, a reservoir was charged with 35 L of dye solution and chemicals, and it was continuously pumped into the CPC reactor. After flowing through all the tubes, solution was again recirculated back to the reservoir.

### 2.3. Analysis

Changes in the Orange II concentration were determined from the absorbance at 480 nm using an UV–vis Spectrophotometer (Zuzi 4418PC). The degree of mineralization was followed by TOC variation. TOC was determined using a TOC-5050 Shimazdu analyser. $H_2O_2$ in solution was determined by titration through

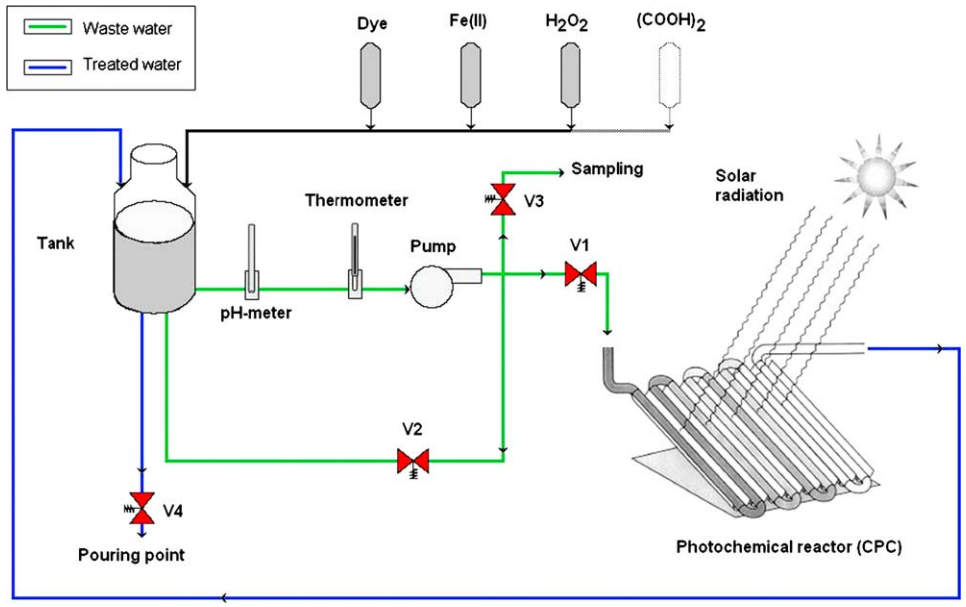


**Fig. 1.** Experimental setup based on a Compound Parabolic Collector Solar Reactor.

an aqueous solution of potassium permanganate (0.02 M) using an automatic Titrino SET/MET 702 (Metrohm). Nitrates and sulphates released from the degradation of OII were determined using a Metrohm ion chromatograph fitted with a 732 IC Conductivity Detector.

### 2.4. Experimental design

The Central Composite Experimental Design was applied to investigate the effect of different variables for the ferrioxalate-assisted solar photo-Fenton process with continuous addition of hydrogen peroxide and air injection (Table 1):

Variables: $H_2O_2$ flow rate, air flow rate, pH and initial concentrations of Fe(II) and oxalic acid.

The design consists of three series of experiments:

(i) a factorial design $2^k$ (all possible combinations of codified values +1 and −1) which in the case of $k = 5$ variables consists of 32 experiments (Experiments 1–32);
(ii) axial of star points (codified values $\alpha = 2^{k/4} = \pm 2.378$) consisting of 2 $k = 10$ experiments (Experiments 33–42);
(iii) central, replicates of the central point (four experiments, 43–46).

Four additional experiments (47–50) were carried out to complete the degradation study. Temperature and incident solar power were not controlled during the experiment, but they were measured during reaction, so that their average values were included in the fitting. It was found that both the initial rates of decoloration and mineralization of Orange II solutions obey pseudo-first order kinetics. The values of $k_d$ (decoloration rate pseudoconstant, $W^{-1}\,h^{-1}$) and $k_{TOC}$ (mineralization rate pseudo-constant, $W^{-1}\,h^{-1}$) were related to the accumulated solar energy received by the water solution.

## 3. Results and discussion

### 3.1. Decoloration and mineralization of dye solutions

As previously reported by the authors [22], Orange II degradation with solar light in the presence of the heterogeneous catalyst $TiO_2$-P-25 with addition of hydrogen peroxide caused 100% decoloration after 30 min and 90% TOC removal in 180 min. Nevertheless, at industrial scale, the use of an homogeneus catalyst such us Fe(II) could offer an economical and practical alternative for the destruction of this environmental contaminant if a ferrous concentration below discharge legal limit (2 ppm) could be used efficiently. The removal or treatment of the sludge of treated wastewater containing excess Fe ions is expensive and the use of chemicals and manpower would be necessary [6,16].

To achieve this goal using a maximum concentration of 2 ppm $Fe^{2+}$ (limit value in treated water to be dumped directly into the environment, according to the European Union Directive), the addition of oxalic acid to the solar photo-Fenton system to form oxalate complexes was previously investigated by our group [14]. In that study, the results revealed than 100% decoloration and 80% of TOC removal of dye solution could be reached by using the ferrioxalate-assisted solar photo-Fenton process.

In this work, the continuous addition of $H_2O_2$ and bubbling of air to the SPFox system (Fe(II)/$H_2O_2$/oxalic acid) irradiated under sunlight could diminish the scavenger effect of excess peroxide and favour the oxidation reactions, respectively. Thus, the mineralization efficiency could be improved.

In all the SPFox experiments, the disappearance of Orange II and the TOC removal followed pseudo-first order kinetics with respect to the dye and Total Organic Carbon concentrations, respectively, as follows:

$$r = -\frac{dC}{di} = kC \tag{9}$$

where "$r$" is the reaction rate, "$C$" the concentration (mg $L^{-1}$) of Orange II or TOC at an accumulated solar energy "$i$" (W h) and "$k$" the pseudo-first order decoloration (namely $k_d$) or mineralization (namely $k_{TOC}$) kinetic rate constant ($W^{-1}\,h^{-1}$) for the photochemical reaction. This equation can be integrated between $i = 0$ and $i = i$, yielding:

$$\ln \frac{C_o}{C} = ki \tag{10}$$

where $C_o$ is the initial concentration of Orange II or TOC. According to this expression, a plot of the first term versus "$i$" must yield a straight line validating Eq. (10) whose slope is $k_d$ or $k_{TOC}$.

To study the effect of the variables peroxide flow rate, air flow rate, pH and initial concentrations of Fe(II) and oxalic acid on the

**Table 1**
The 5-factor Central Composite Design Matrix and the values of the response functions, $k_d$ and $k_{TOC}$. Ferrioxalate-assisted solar photo-Fenton system with continuous addition of peroxide and air injection.

| Ferrioxalate-assisted solar photo-Fenton system with continuous addition of peroxide and air injection, [dye] = 20 ppm | | | | | | | | | |
|---|---|---|---|---|---|---|---|---|---|
| EXP. | $H_2O_2$ flow (ml $min^{-1}$) | [Fe(II)] (ppm) | Air flow ($m^3$ $h^{-1}$) | [$H_2C_2O_4$] (ppm) | pH | $k_d$ ($W^{-1}$ $h^{-1}$) | $k_{TOC}$ ($W^{-1}$ $h^{-1}$) | $T^*$(°C) | Solar power* (W $m^{-2}$) |
| 1 | 0.71 | 7.10 | 1.31 | 42.61 | 4.84 | 0.500 | 0.161 | 23.2 | 27.2 |
| 2 | 0.29 | 7.10 | 1.31 | 42.61 | 4.84 | 0.077 | 0.004 | 20.2 | 41.26 |
| 3 | 0.71 | 2.90 | 1.31 | 42.61 | 4.84 | 0.027 | 0.003 | 24.4 | 29.14 |
| 4 | 0.29 | 2.90 | 1.31 | 42.61 | 4.84 | 0.048 | 0.007 | 21.8 | 32.56 |
| 5 | 0.71 | 7.10 | 0.89 | 42.61 | 4.84 | 0.175 | 0.025 | 21.2 | 33.18 |
| 6 | 0.29 | 7.10 | 0.89 | 42.61 | 4.84 | 0.038 | 0.006 | 24.2 | 35.82 |
| 7 | 0.71 | 2.90 | 0.89 | 42.61 | 4.84 | 0.029 | 0.005 | 20.0 | 35.88 |
| 8 | 0.29 | 2.90 | 0.89 | 42.61 | 4.84 | 0.011 | 0.007 | 24.2 | 36.36 |
| 9 | 0.71 | 7.10 | 1.31 | 17.39 | 4.84 | 0.018 | 0.004 | 21.4 | 40.68 |
| 10 | 0.29 | 7.10 | 1.31 | 17.39 | 4.84 | 0.040 | 0.003 | 21.6 | 45.12 |
| 11 | 0.71 | 2.90 | 1.31 | 17.39 | 4.84 | 0.026 | 0.003 | 22.0 | 45.50 |
| 12 | 0.29 | 2.90 | 1.31 | 17.39 | 4.84 | 0.011 | 0.001 | 24.2 | 42.62 |
| 13 | 0.71 | 7.10 | 0.89 | 17.39 | 4.84 | 0.012 | 0.004 | 23.0 | 44.62 |
| 14 | 0.29 | 7.10 | 0.89 | 17.39 | 4.84 | 0.028 | 0.004 | 24.4 | 37.66 |
| 15 | 0.71 | 2.90 | 0.89 | 17.39 | 4.84 | 0.006 | 0.013 | 22.6 | 45.00 |
| 16 | 0.29 | 2.90 | 0.89 | 17.39 | 4.84 | 0.013 | 0.003 | 23.0 | 45.28 |
| 17 | 0.71 | 7.10 | 1.31 | 42.61 | 3.16 | 0.466 | 0.089 | 23.6 | 36.28 |
| 18 | 0.29 | 7.10 | 1.31 | 42.61 | 3.16 | 0.303 | 0.075 | 25.6 | 45.28 |
| 19 | 0.71 | 2.90 | 1.31 | 42.61 | 3.16 | 0.509 | 0.072 | 25.6 | 44.84 |
| 20 | 0.29 | 2.90 | 1.31 | 42.61 | 3.16 | 0.364 | 0.073 | 23.6 | 28.62 |
| 21 | 0.71 | 7.10 | 0.89 | 42.61 | 3.16 | 0.492 | 0.083 | 20.1 | 33.56 |
| 22 | 0.29 | 7.10 | 0.89 | 42.61 | 3.16 | 0.472 | 0.120 | 24.6 | 34.36 |
| 23 | 0.71 | 2.90 | 0.89 | 42.61 | 3.16 | 0.532 | 0.066 | 26.4 | 43.76 |
| 24 | 0.29 | 2.90 | 0.89 | 42.61 | 3.16 | 0.362 | 0.056 | 27.0 | 45.84 |
| 25 | 0.71 | 7.10 | 1.31 | 17.39 | 3.16 | 0.468 | 0.106 | 26.2 | 33.24 |
| 26 | 0.29 | 7.10 | 1.31 | 17.39 | 3.16 | 0.450 | 0.080 | 26.4 | 28.60 |
| 27 | 0.71 | 2.90 | 1.31 | 17.39 | 3.16 | 0.526 | 0.062 | 24.0 | 30.18 |
| 28 | 0.29 | 2.90 | 1.31 | 17.39 | 3.16 | 0.254 | 0.040 | 23.6 | 49.68 |
| 29 | 0.71 | 7.10 | 0.89 | 17.39 | 3.16 | 0.475 | 0.107 | 24.4 | 33.82 |
| 30 | 0.29 | 7.10 | 0.89 | 17.39 | 3.16 | 0.464 | 0.103 | 20.4 | 30.98 |
| 31 | 0.71 | 2.90 | 0.89 | 17.39 | 3.16 | 0.527 | 0.051 | 23.0 | 45.7 |
| 32 | 0.29 | 2.90 | 0.89 | 17.39 | 3.16 | 0.262 | 0.033 | 23.4 | 45.62 |
| 33 | 1.00 | 5.00 | 1.10 | 30.00 | 4.00 | 0.485 | 0.038 | 24.8 | 36.84 |
| 34 | 0.00 | 5.00 | 1.10 | 30.00 | 4.00 | 0.504 | 0.074 | 26.0 | 42.26 |
| 35 | 0.50 | 10.00 | 1.10 | 30.00 | 4.00 | 0.159 | 0.059 | 26.1 | 45.04 |
| 36 | 0.50 | 0.00 | 1.10 | 30.00 | 4.00 | 0.029 | 0.003 | 25.6 | 45.16 |
| 37 | 0.50 | 5.00 | 1.60 | 30.00 | 4.00 | 0.503 | 0.051 | 24.4 | 35.28 |
| 38 | 0.50 | 5.00 | 0.60 | 30.00 | 4.00 | 0.508 | 0.037 | 24.6 | 42.84 |
| 39 | 0.50 | 5.00 | 1.10 | 60.00 | 4.00 | 0.229 | 0.034 | 24.8 | 45.44 |
| 40 | 0.50 | 5.00 | 1.10 | 0.00 | 4.00 | 0.122 | 0.029 | 24.6 | 45.06 |
| 41 | 0.50 | 5.00 | 1.10 | 30.00 | 6.00 | 0.030 | 0.014 | 25.4 | 45.86 |
| 42 | 0.50 | 5.00 | 1.10 | 30.00 | 2.00 | 0.324 | 0.035 | 24.4 | 39.26 |
| 43 | 0.50 | 5.00 | 1.10 | 30.00 | 4.00 | 0.282 | 0.043 | 24.0 | 45.98 |
| 44 | 0.50 | 5.00 | 1.10 | 30.00 | 4.00 | 0.273 | 0.042 | 25.8 | 42.12 |
| 45 | 0.50 | 5.00 | 1.10 | 30.00 | 4.00 | 0.288 | 0.047 | 26.2 | 45.94 |
| 46 | 0.50 | 5.00 | 1.10 | 30.00 | 4.00 | 0.277 | 0.045 | 26.4 | 44.89 |
| Codified levels | | | | | | | | | |
| (+α) | 1.00 | 10.00 | 1.60 | 60.00 | 6.00 | | | | |
| (−α) | 0.00 | 0.00 | 0.60 | 0.00 | 2.00 | | | | |
| (+1) | 0.71 | 7.10 | 1.31 | 42.61 | 4.84 | | | | |
| (−1) | 0.29 | 2.90 | 0.89 | 17.39 | 3.16 | | | | |
| (0) | 0.50 | 5.00 | 1.10 | 30.00 | 4.00 | | | | |
| Additional experiments | | | | | | | | | |
| 47[a] | 0.50 | 5.00 | 0.00 | 30.00 | 4.00 | 0.516 | 0.083 | 26.8 | 44.26 |
| 48[b] | 0.50 | 0.00 | 0.00 | 0.00 | 4.00 | – | – | 27.2 | 42.58 |
| 49[c] | 0.00 | 0.00 | 0.00 | 0.00 | 0.00 | 0.000 | 0.000 | 29.1 | 35.82 |
| 50[d] | 0.50 | 5.00 | 1.10 | 30.00 | 4.00 | 0.176 | 0.000 | 32.0 | 45.01 |

[a] Without air injection.
[b] Without dye.
[c] Only dye.
[d] In presence of 0.1 M *tert*-butylalcohol.
* Average temperature ($T$) and incident solar power.

two response functions (kinetic decoloration and mineralization rate constants), a Central Composite Design was performed. The Central Composite Design Matrix (Table 1) shows the operation conditions (factors values) and the obtained $k_d$ and $k_{TOC}$ values. The temperature and solar power were not controlled during the experiment, but they were measured during reaction, so their average values were included in the fitting. In all photodegradation experiments, the temperature and solar power varied between 20

and 32 °C and between 25 and 45 W $m^{-2}$, respectively. Experimental results and NNs fittings of these constants are shown in Fig. 2 and are in good agreement, with an average error lower than 11% and 15% for dye solutions decoloration and mineralization, respectively. The equations and parameters for the fitting of $k_d$ and $k_{TOC}$ using NNs are shown in Table 2. $N_1$ and $N_2$ are general factors related to the first and the second neuron, respectively. $W_{11}$–$W_{17}$ are the contribution parameters to the first neuron and represent the influence of each of the seven factors in the process. $W_{21}$–$W_{27}$ are the contributions to the second neuron and are related to the same factors. From these results it is possible to deduce the effect of each parameter on the response functions.

The results of a saliency analysis on the input variables for each neural network (%) are shown in Table 3. It is confirmed that pH and flow rate of hydrogen peroxide are the most significant factors affecting the decoloration kinetics whereas the air flow rate, solar power and temperature are the most significant variables affecting the mineralization kinetics, as will be explained below.

### 3.1.1. Effect of pH and $H_2O_2$ flow rate

The equations shown in Table 2 allow a simulation analysis of the effect of any of the studied variables on the values of $k_d$ and $k_{TOC}$. For example, the influence of the pH and $H_2O_2$ flow rate on $k_d$ is represented in three dimensions in Fig. 3a. pH is an important parameter for photo-Fenton processes. It affects the generation of hydroxyl radicals and the nature of iron species in solution. The results presented in Table 3 showed that Orange II solutions decoloration should depend strongly on the pH and $H_2O_2$ flow rate values. As shown in Fig. 3a, the OII solutions decoloration under the SPFox system with continuous addition of $H_2O_2$ and air injection is favoured at pHs between 2.0 and 4.5. In this range of pH, in the ferrioxalate system, the predominant species are $Fe(C_2O_4)_2^{2-}$ and $Fe(C_2O_4)_3^{3-}$ (Fig. 3b, [23]), with a photoreactivity higher than $FeC_2O_4^+$, and under solar UV light they can effectively convert $Fe^{3+}$ ion into $Fe^{2+}$ ion by Eq. (1), being more hydroxyl radicals generated by reaction of generated ferrous ions with hydrogen peroxide [24]. On the other hand, above this optimum pH, the process efficiency decreases since the Fe(III) complexes coagulation reduces the catalyst effect of Fe(II) to decompose $H_2O_2$ [25]. The $H_2O_2$ dosage has a positive effect on decoloration until pH 4.5. Above this pH, when $Fe(C_2O_4)_3^{3-}$ present in solution is irradiated with UV light generates $H_2O_2$ according to Eqs. (1)–(5) and hydroxyl radical scavenger effect can be produced. An excess of hydrogen peroxide reduces catalytic activity since it favours reaction (7) diminishing the amount of $^{\bullet}OH$ radicals available to destroy Orange II. Although other radicals are produced ($HO_2^{\bullet}$), their oxidation potential is much smaller than that of the hydroxyl radicals. Additionally, decomposition of $H_2O_2$ to form water and oxygen is also favoured according to Eqs. (5), (7) and (8), as indicated above.

When the pH value increases up to 6, the $Fe^{3+}$ and $Fe^{2+}$ species cannot almost exist in the wastewater and the predominant specie of Fe was $Fe(OH)_3$ as the precipitate, which might hardly be photoactive and cannot be regenerated to the ferrous ion, in agreement with other authors [26].

Under the operation conditions shown in Fig. 3a, the maximum decoloration constant, $k_d$, was approximately 0.47 $W^{-1}$ $h^{-1}$ at pHs 2.5–3, while in the system without continuous addition of peroxide nor air injection, the maximum obtained value of $k_d$ was 0.23 $W^{-1}$ $h^{-1}$ [14], which indicates the decrease of scavenger effect in the present system. In both systems, 100% decoloration was attained but with different reaction rates.

Regarding OII solutions mineralization (data not shown), pH values between 2 and 4.5 are also required since high hydroxyl radical concentrations are necessary to destroy the benzene and naphthalene groups. The best obtained degradation result was a

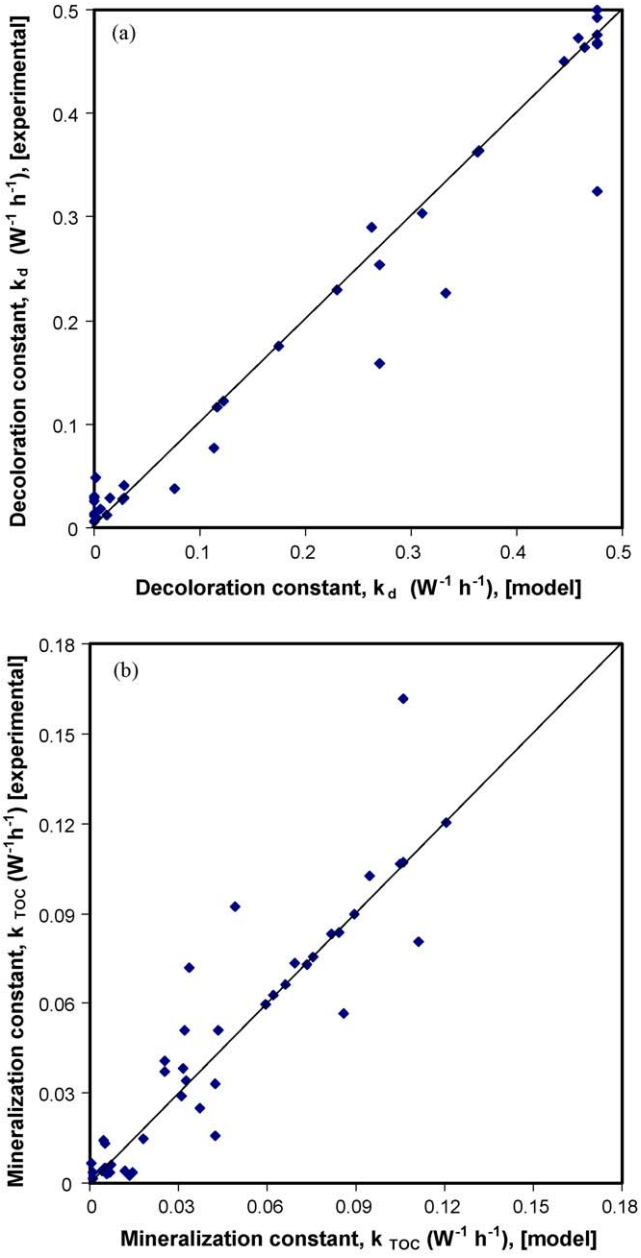


**Fig. 2.** Neural network fittings of Ferrioxalate-assisted solar photo-Fenton system with continuous addition of $H_2O_2$ and air injection; (a) decoloration rate pseudoconstant; (b) mineralization rate pseudoconstant.

TOC removal of 95% versus 80% reached in the SPFox system with addition of $H_2O_2$ at the beginning of reaction [14].

### 3.1.2. Effect of air and $H_2O_2$ flow rates at different ferrous concentrations

The mineralization results shown in Fig. 4 revealed that continuous addition of $H_2O_2$ and air bubbled to the SPFox system (Fe(II)/$H_2O_2$/oxalic acid process irradiated under sunlight) could increase the reaction rates or cause inhibition effects depending on operation conditions. Thus, if the reaction was conduced only using the initial amount of 75 ppm $H_2O_2$, without continuous addition of hydrogen peroxide and without air injection, the increase of initial ferrous concentration do not improve the mineralization degree (≈60–75% TOC removal). That happened because although Fe(II) can accelerate the decomposition of $H_2O_2$ to form hydroxyl radicals, the amount of $H_2O_2$ added at the beginning of the reaction

**Table 2**
Equation and parameters of neural network fittings for Orange II solutions decoloration and mineralization under the process: Ferrioxalate-assisted solar photo-Fenton with continuous addition of hydrogen peroxide and air injection.

| Neural network fitting | | |
|---|---|---|
| Equation* | Decoloration | |
| $k_d$ [$W^{-1}\,h^{-1}$] = $N_1 \times (1/(1 + 1/EXP([H_2O_2$ flow] $\times W_{11}$ + [Fe] $\times W_{12}$ + [pH] $\times W_{13}$ + [$H_2C_2O_4$] $\times W_{14}$ + [Temperature] $\times W_{15}$ + [Solar power] $\times W_{16}$ + [Air flow] $\times W_{17}$))) + $N_2 \times (1/(1 + 1/EXP([H_2O_2$ flow] $\times W_{21}$ + [Fe] $\times W_{22}$ + [pH] $\times W_{23}$ + [$H_2C_2O_4$] $\times W_{24}$ + [Temperature] $\times W_{25}$ + [Solar Power] $\times W_{26}$ + [Air flow] $\times W_{27}$))) | | |
| Weight factors | Parameter | Values of neurons and factors to obtain the decoloration kinetic rate constant of dye solutions, $k_d$. |
| $N_1$ | *Neuron* | 0.2627 |
| $W_{11}$ | $H_2O_2$ flow | 2.3347 |
| $W_{12}$ | [Fe(II)] | 10.8466 |
| $W_{13}$ | pH | −21.5796 |
| $W_{14}$ | [$H_2C_2O_4$] | 10.6664 |
| $W_{15}$ | Temperature | 0.1497 |
| $W_{16}$ | Solar Power | 0.2129 |
| $W_{17}$ | Air flow | 2.5082 |
| $N_2$ | *Neuron* | 0.2139 |
| $W_{21}$ | $H_2O_2$ flow | 27.2670 |
| $W_{22}$ | [Fe(II)] | 2.0658 |
| $W_{23}$ | pH | −25.3600 |
| $W_{24}$ | [$H_2C_2O_4$] | 6.3131 |
| $W_{25}$ | Temperature | 0.4259 |
| $W_{26}$ | Solar power | −4.5553 |
| $W_{27}$ | Air flow | −4.5689 |
| Equation* | Mineralization | |
| $k_{TOC}$ [$W^{-1}\,h^{-1}$] = $N_1 \times (1/(1 + 1/EXP([H_2O_2$ flow] $\times W_{11}$ + [Fe] $\times W_{12}$ + [pH] $\times W_{13}$ + [$H_2C_2O_4$] $\times W_{14}$ + [Temperature] $\times W_{15}$ + [Solar power] $\times W_{16}$ + [Air flow] $\times W_{17}$))) + $N_2 \times (1/(1 + 1/EXP([H_2O_2$ flow] $\times W_{21}$ + [Fe] $\times W_{22}$ + [pH] $\times W_{23}$ + [$H_2C_2O_4$] $\times W_{24}$ + [Temperature] $\times W_{25}$ + [Solar power] $\times W_{26}$ + [Air flow] $\times W_{27}$))) | | |
| Weight factors | Parameter | Values of neurons and factors to obtain the mineralization kinetic rate constant of dye solutions, $k_{TOC}$. |
| $N_1$ | *Neuron* | −0.9011 |
| $W_{11}$ | $H_2O_2$ flow | −0.8747 |
| $W_{12}$ | [Fe(II)] | 1.9082 |
| $W_{13}$ | pH | 1.0783 |
| $W_{14}$ | [$H_2C_2O_4$] | −0.4304 |
| $W_{15}$ | Temperature | 2.1388 |
| $W_{16}$ | Solar power | −3.1192 |
| $W_{17}$ | Air flow | −3.1905 |
| $N_2$ | *Neuron* | 1.0491 |
| $W_{21}$ | $H_2O_2$ flow | −0.6639 |
| $W_{22}$ | [Fe(II)] | 1.7912 |
| $W_{23}$ | pH | 0.1162 |
| $W_{24}$ | [$H_2C_2O_4$] | −0.0745 |
| $W_{25}$ | Temperature | 2.0332 |
| $W_{26}$ | Solar power | −2.6470 |
| $W_{27}$ | Air flow | −2.7593 |

* Parameters values in equations must be previously normalized to the (0.1) interval.

was not enough to generate more $^{\bullet}OH$ radicals necessary to achieve the total mineralization. In this case, the remaining $H_2O_2$ concentration in solution was negligible after 50 W h received by the water solution. On the other hand, at ferrous concentrations greater than 10 ppm (data not shown), an inhibition effect was presented due to Fe(II) competing different radicals with dye molecules as it is shown in Eqs. (11)–(13):

$$Fe(II) + {}^{\bullet}OH \rightarrow Fe(III) + OH^{-} \quad (11)$$

$$Fe(II) + HO_2{}^{\bullet} \rightarrow Fe(III)(HO_2)^{+2} \quad (12)$$

$$Fe(II) + O_2{}^{\bullet -} + H^{+} \rightarrow Fe(III)(HO_2)^{+2} \quad (13)$$

It can also been shown from Fig. 4 that the air flow rate affects positively to the photocatalytic reaction until an optimal value of air flow was used, but only when used ferrous initial concentration was greater than 5 ppm, and this optimal air flow value diminished as the $H_2O_2$ flow rate increased. When the

**Table 3**
Saliency analysis of the input variables for the neural network (%).

| Neural network output | Parameters | | | | | | |
|---|---|---|---|---|---|---|---|
| | $H_2O_2$ flow | [Fe] | pH | [$H_2C_2O_4$] | Temperature | Solar power | Air flow |
| Decoloration kinetic rate constant, $k_d$ ($W^{-1}\,h^{-1}$) | 21.74 | 12.69 | 40.31 | 15.52 | 0.46 | 3.45 | 5.83 |
| Mineralization kinetic rate constant, $k_{TOC}$ ($W^{-1}\,h^{-1}$) | 6.72 | 16.37 | 4.81 | 2.06 | 18.47 | 25.36 | 26.20 |

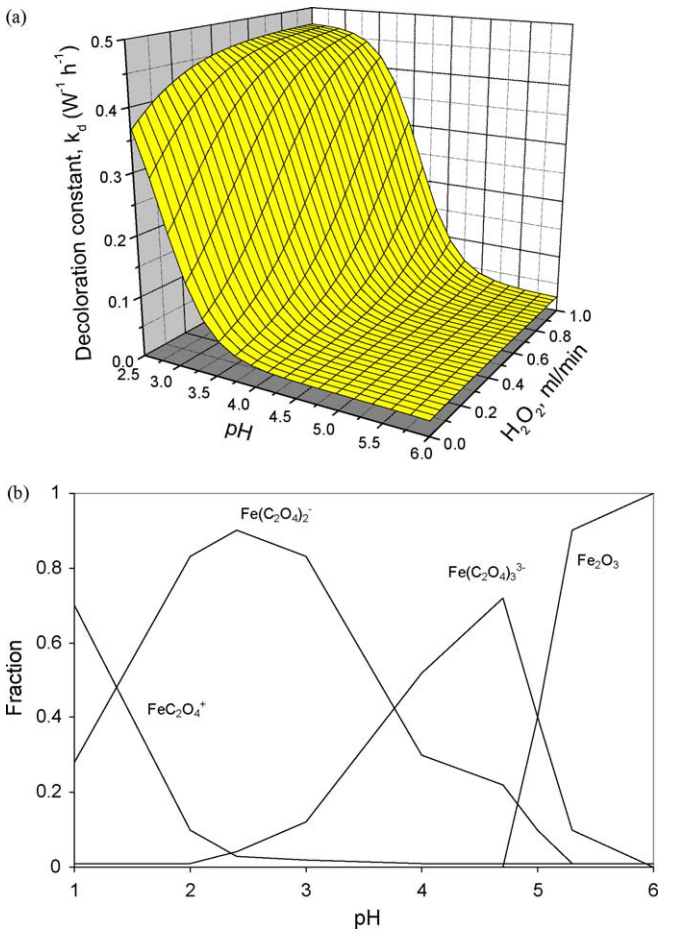


**Fig. 3.** (a) NNs simulation of the effect of pH and $H_2O_2$ flow rate on Orange II solutions decoloration constant, $k_d$. [Orange II] = 20 ppm; [Fe(II)] = 2 ppm; $[H_2C_2O_4]$ = 60 ppm; air flow rate: 1.3 $m^3$ $h^{-1}$; accumulated solar energy: 50 W h; average temperature: 24 °C; (b) fraction of species of Fe(III) as a function of pH.

initial concentration of Fe(II) increases the decomposition of hydrogen peroxide increases and a higher flow of air can be bubbled into the reactor without inhibit the reaction. As it can be seen from Fig. 4c, the increase of air flow (below optimal value) increases the mineralization constant since the oxygen in the reaction medium avoids the auto-decomposition of $H_2O_2$ in $H_2O$ and $O_2$ and more hydrogen peroxide can produce more hydroxyl radicals. Besides, the effect of the peroxide dosage was positive below this optimal air flow but inhibited the mineralization reaction when an air excess was used (•OH scavenger effect). It is important to point out that when ferrous concentrations below discharge levels (2 ppm) were used, the effect of peroxide flow rate only was positive if no injection of air was done. This system presents this advantage since it permits the use of an Fe(II) initial concentration of 2 ppm, and so injection of air would not be necessary (Fig. 4a), and under the optimal conditions, 100% decoloration and 95% mineralization of dye solutions can be reached. Thus, in this process, the operation costs of Fe removal and electric power are reduced.

### 3.1.3. Effect of oxalic initial concentration

Over the studied range, oxalic acid positively affects (data not shown) to the degradation reaction under the SPFox system with continuous addition of $H_2O_2$ until an optimal value of oxalic is used, in agreement with data previously reported by the authors [14]. It is due to the faster generation of $Fe^{2+}$ ion by photolysis of ferrioxalate and additional hydroxyl radicals produced (Eqs. (1)–(6)). The photolysis of ferrioxalate in the presence of hydrogen peroxide is a continuous source of Fenton's reagent.

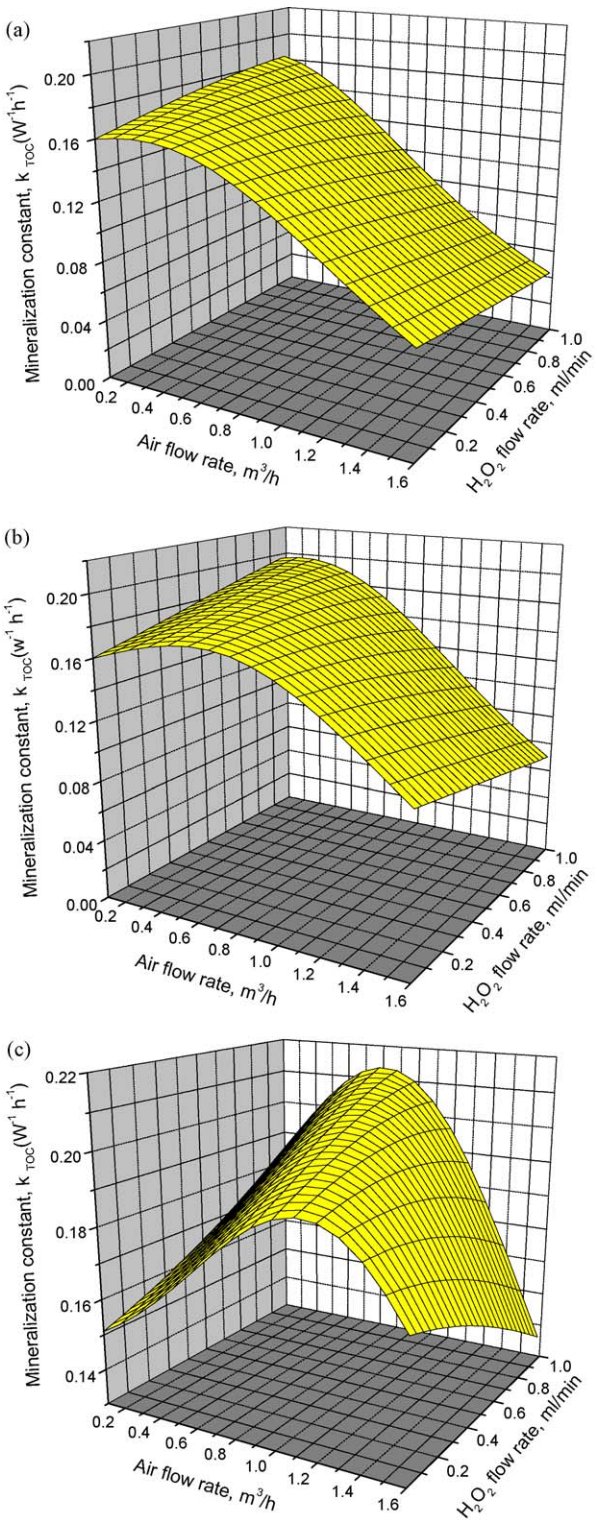


**Fig. 4.** NNs simulation of the effect of the air and $H_2O_2$ flow rates on Orange II solutions mineralization constant, $k_{TOC}$. [Orange II] = 20 ppm; pH 2; accumulated solar energy = 50 W h; $[(H_2C_2O_4)]$ = 30 ppm. (a) [Fe(II)] = 2 ppm; (b) [Fe(II)] = 5 ppm; (c) [Fe(II)] = 10 ppm.

On the other hand, the TOC removal efficiency increased with the $[H_2C_2O_4]$/[Fe] molar ratio up to 3, beyond which it declined, because at an $[H_2C_2O_4]$/[Fe] molar ratio of 3, the Fe(III) ions were complexed with the maximum amount of oxalate, in the form of

the saturated complex $Fe(C_2O_4)_3^{3-}$ (ferric complexed with three oxalate molecules as its limit load). However, when the molar ratio is below 3, insufficient oxalate amount is present, and some of the ferric ions can precipitate as $Fe(OH)_3$, reducing the yield of $Fe^{2+}$ ion regeneration. Besides, the efficiency decreased as molar ratio increased $[H_2C_2O_4]/[Fe] > 3$, possibly due to the excess oxalate cannot complex with more ferric ions in solution and the light penetration through irradiated wastewater decreases. In addition, the excess of oxalate acts as an additional organic compound and so competes the •OH radicals with the Orange II reducing the decoloration efficiency. This is in agreement with data reported by others authors about degradation of reactive Black B in a photo/ferrioxalate system [27]. On the other hand, the negative effect on the mineralization of dye solution with excess of oxalic acid can be also due to $CO_2$ produced according to Eq. (3) could be converted to $CO_3^{2-}$ or $HCO_3^-$ at acid pH, which may scavenge the hydroxyl radicals and so to decrease the degradation efficiency.

Thus, the addition of oxalic acid to degrade the Orange II solution cannot only improve the degradation reaction, but oxalic acid may also be used to adjust the pH of dye solution and reduce the operation costs.

### 3.1.4. Effect of temperature

The temperature of Orange II solution in different experiments varied from 20 to 32 °C, and two opposite effects were presented. This parameter always led to an increasing reaction rates according to the Arrhenius law. However, on one hand, temperature likely increased the •OH radicals generation by decomposition of $H_2O_2$ and by other equations indicated above. Simultaneously, on the other hand, temperature also influences the inefficient decomposition of hydrogen peroxide into $H_2O$ and $O_2$ (inactive species) and the formation of radicals with smaller oxidation potential. The obtained results in this work (data not shown) revealed that from 20 to 29 °C, degradation reaction rate increased since the enhancement of •OH species generation prevails over the inefficient species formation, but a further temperature increase, to 32 °C, decreases the photodegradation efficiency.

### 3.1.5. Radical or molecular pathway study

To study molecular and/or radical reactions, scavenging of hydroxyl radicals was accomplished by using 0.1 M *tert*-butylalcohol. The obtained results of the reactions of Orange II degradation with or without *tert*-butylalcohol are shown in Table 4. As it can be seen, when the photodegradation reaction was carried out by using solar radiation as the only oxidizing agent, both decoloration and mineralization degree were negligible. If the reaction combines solar light and oxidant $H_2O_2$, only total decoloration is attained (•OH radicals concentration generated under these conditions is negligible) due to hydrogen peroxide reacts primarily as the $H_2O_2$ molecule with the chromophore group by selective and relatively slow reaction ($k_d = 0.18\ W^{-1}\ h^{-1}$). Decoloration reaction rate increases by the addition of Fe(II) and oxalic acid to the solar/$H_2O_2$ system (SPFox system with continuous addition of $H_2O_2$, $k_d = 0.475\ W^{-1}\ h^{-1}$) due to $H_2O_2$ and ferrioxalate complexes rapidly decomposes into hydroxyl free radicals which also react with the azo (N=N) linkage (≈50% importance molecular pathway and ≈50% radical pathway on

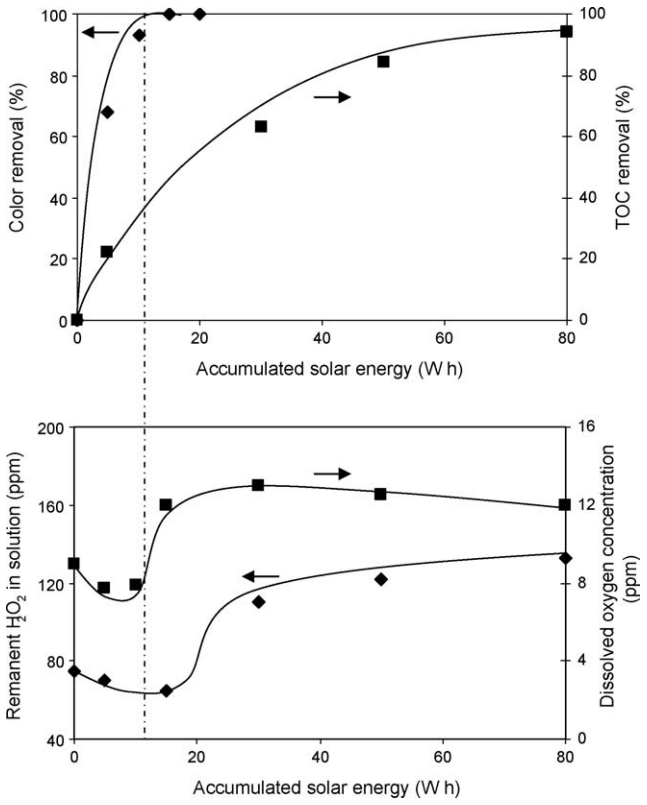


**Fig. 5.** Evolution of TOC and Color removal versus remaining $H_2O_2$ and dissolved oxygen concentrations along the photodegradation reaction. [Orange II] = 20 ppm; [Fe(II)] = 2 ppm; $[H_2C_2O_4]$ = 60 ppm; air flow rate: 1.3 $m^3\ h^{-1}$; accumulated solar energy: 80 W h; $H_2O_2$ flow rate: 0.5 ml $min^{-1}$; pH 3; average temperature: 24 °C.

decoloration reaction). Besides, the obtained results suggest that these •OH radicals play a significant role in the mineralization of Orange II solutions, being 95% TOC removal reached (100% radical pathway) without radical scavenger. On the other hand, 0% TOC removal was attained in the presence of *tert*-butylalcohol. It can be concluded that the radical oxidation pathway represents over the 50% of the overall decoloration reaction and 100% of mineralization process when the SPFox system with continuous addition of $H_2O_2$ was developed.

### 3.1.6. Description of an example experiment

From Fig. 5, it can be concluded the following: In all photodegradation experiments under the SPFox system with continuous addition of $H_2O_2$ and air injection, in a first stage, both remaining $H_2O_2$ and dissolved $O_2$ concentrations decrease during decoloration phase reaching a minimum value when total decoloration was attained. Ferrous ions react very quickly with hydrogen peroxide (Eq. (6)) to produce hydroxyl radicals which preferentially attack and breakdown the azo double bond (N=N) in the chromophore group. Oxygen is mainly consumed by Eq. (3) that prevails over the oxygen generation by Eq. (5). 100% of dye solution decoloration was obtained by both molecular oxidation pathway with $H_2O_2$ as oxidant and radical pathway mainly with

**Table 4**
Radical and/or molecular reaction pathway study.

| System | $k_d$ ($W^{-1}\ h^{-1}$) | Color removal (%) | $k_{TOC}$ ($W^{-1}\ h^{-1}$) | TOC removal (%) |
|---|---|---|---|---|
| Solar | 0.001 | 11 (50 W h) | 0.0004 | 4 (50 W h) |
| Solar/$H_2O_2$ | 0.180 | 100 (50 W h) | 0.0000 | 0 |
| SPFox/continuous addition of $H_2O_2$ | 0.475 | 100 (20 W h) | 0.1600 | 95 (50 W h) |
| SPFox/continuous addition of $H_2O_2$/*tert*-butylalcohol | 0.176 | 100 (50 W h) | 0.0000 | 0 |

•OH species. Until this moment, only 30% TOC removal was achieved.

In a second stage, once color has disappeared, •OH radicals attack the benzene and naphthalene rings of OII molecule and intermediate compounds formed from the dye decomposition. Analysis of the UV–vis absorption spectra of Orange II before and after oxidation (absorbance reduction data at 40 W h: naphthalene (70%) and benzene (55%)) allows to conclude that naphthalene ring is broken sooner than benzene ring. It must be remarked that in this stage, $H_2O_2$ and $O_2$ in solution also increased possibly due to their generation by Eqs. (5) and (17).

TOC reduction is due to the decarboxylation of organic-acid intermediates [28]:

$$[Fe(III)(RCO_2)^-]^{+2} + h\nu \rightarrow Fe(II) + CO_2 + R^\bullet \quad (14)$$

Based on our results of dye degradation by the ferrioxalate-assisted solar photo-Fenton process and according to Feng et al. [29], the overall stoichiometry for the mineralization of Orange II can be written by Eq. (15), taking also into account mainly Eqs. (1), (16) and (17):

$$C_{16}H_{11}N_2NaO_4S + 42H_2O_2 \rightarrow 16CO_2 + 46H_2O + 2HNO_3 + NaHSO_4 \quad (15)$$

$$Fe(III) + H_2O \rightarrow Fe(III)(HO_2)^{+2} + H^+ \quad (16)$$

$$Fe(III) + O_2^{\bullet -} \rightarrow Fe(II) + O_2 \quad (17)$$

On the basis of Eq. (15), 42 mol of $H_2O_2$ are theoretically needed to completely degrade 1 mol of Orange II, which produces 2 mol of $HNO_3$ and 1 mol of $NaHSO_4$. In our case, 80 ppm $H_2O_2$ are required to mineralization of 20 ppm Orange II, optimal molar ratio [$H_2O_2$]/[Orange II] equals 41, that is only slightly lower than the theoretical value (95% TOC removal is attained). When the degradation reaction was carried out under the SPFox system with addition of $H_2O_2$ at the beginning of reaction [14], the optimal ratio [$H_2O_2$]/[Orange II] was equals 45, which indicates the increase of the photodegradation efficiency in this present system. On the other hand, according to Eq. (15), the mineralization of 20 ppm of Orange II produces 7 ppm nitrate and 5.5 ppm sulphate. In our case, 6.6 ppm nitrate and 5.2 ppm sulphate were obtained, that is in agreement with the 95% TOC removal achieved.

It is important to point out that these results were obtained using 2 ppm of ferrous ion (discharge legal limit), without air injection and using oxalic acid, which reduces the costs of electric power, chemicals and of removal of Fe ions at the end of treatment.

## 4. Conclusions

Degradation of Orange II solutions developed in a Compound Parabolic Collector under ferrioxalate-assisted solar photo-Fenton systems, using ferrous initiated processes, allows a continuous treatment of waste water being an industrially feasible technique. Results showed that the continuous addition of $H_2O_2$ to the waste water during irradiation has been found to contribute to the increase of the overall efficiency of the process. A comparative study shows that 100% decoloration of dye solution can be reached by using the SPFox system with addition of $H_2O_2$ at the beginning or along the reaction but with different irradiation times. However, the efficiency of TOC removal (95%) was higher in the SPFox with peroxide continuous dosage. In addition, the solar photo-Fenton degradation with oxalic acid is efficient and permits the use of a concentration of 2 ppm Fe(II) (below discharge criterion according to European Union) and in this case, air bubbling would not be necessary. Oxalic acid can also be used to pH adjustment, reducing the operation costs of Fe removal, chemicals and manpower.

This process can be considered environmentally friendly since it is composed only of atoms of hydrogen, oxygen and carbon, yielding water, $CO_2$ and hydroxyl ions as desirable final products.

## Acknowledgement

Financial support from the Programa de Ciencias y Tecnologías Químicas (Junta de Comunidades de Castilla-La Mancha, Spain (PCI08-0047-4810) is gratefully acknowledged.

## References

[1] R.F.P. Nogueira, M.R.A. Silva, A.G. Trovó, Sol. Energy 79 (2005) 384–392.
[2] J. Feng, X. Hu, P.L. Yue, H.Y. Zhu, G.Q. Lu, Water Res. 37 (2003) 3776–3784.
[3] J. Pignatello, Environ. Sci. Technol. 26 (1992) 944–951.
[4] M. Pérez, F. Torrades, X. Domenech, J. Peral, Water Res. 36 (2002) 2703–2710.
[5] D. Robert, A. Piscopo, J.V. Weber, Sol. Energy 77 (2004) 553–558.
[6] D. Gumy, P. Fernández-Ibañez, S. Malato, C. Pulgarín, O. Enea, J. Kiwi, Catal. Today 101 (2005) 375–382.
[7] P.L. Huston, J.J. Pignatello, Water Res. 33 (1999) 1238–1246.
[8] R.F.P. Nogueira, J.R. Guimarães, Water Res. 34 (2000) 895–901.
[9] C.A. Emilio, W.F. Jardim, M.L. Litter, H.D. Mansilla, J. Photochem. Photobiol. A 151 (2002) 121–127.
[10] G.D. Copper, G.D. DeGraff, J. Phys. Chem. 76 (1972) 2618–2625.
[11] D.L. Sedlak, J. Hoigné, Atmos. Environ. 27 (1993) 2173–2185.
[12] Y.G. Zuo, Geochim. Cosmochim. Acta 59 (1995) 3123–3130.
[13] K. Selvam, M. Muruganandham, M. Swaminathan, Sol. Energy Mater. Sol. Cells 89 (2005) 61–74.
[14] J.M. Monteagudo, A. Durán, C. López-Almodovar, Appl. Catal., B: Environ. 83 (2008) 46–55.
[15] J. Feng, X. Hu, P.L. Yue, Environ. Sci. Technol. 38 (2004) 5773–5778.
[16] S. Sabhi, J. Kiwi, Water Res. 35 (2001) 1994–2002.
[17] G.E.P. Box, W.G. Hunter, J.S. Hunter, Statistics for Experimenters: An Introduction to Design, Data Analysis and Model Building, Ed., Wiley, New York, 1978.
[18] D.P. Morgan, C.L. Scofield, Neural networks and Speech Processing, Kluwver Academic Publishers, London, 1991.
[19] R. Nath, B. Rajagopalan, R. Ryker, Comput. Oper. Res. 24 (1997) 767–773.
[20] A. Durán, J.M. Monteagudo, M. Mohedano, Appl. Catal., B: Environ. 65 (2006) 127–134.
[21] A. Durán, J.M. Monteagudo, E. Amores, Appl. Catal., B: Environ 80 (2008) 42–50.
[22] J.M. Monteagudo, A. Durán, Chemosphere 65 (2006) 1242–1248.
[23] Y. Chen, F. Wu, Y. Lin, N. Deng, N. Bazhin, E. Glebov, J. Hazard. Mater. 148 (2007) 360–365.
[24] L. Vineze, S. Papp, Environ. Sci. Technol. 33 (1999) 2418–2424.
[25] H. Zheng, Y. Pan, X. Xiang, J. Hazard. Mater. 141 (2007) 457–464.
[26] F.B. Li, X.Z. Li, X.M. Li, T.X. Liu, J. Dong, J. Colloid Interface Sci. 311 (2007) 481–490.
[27] Y.H. Huang, S.T. Tsai, Y.F. Huang, C.Y. Chen, J. Hazard. Mater. 140 (2007) 382–388.
[28] J.G. Sagawe, A. Lehnard, M. Lübber, D. Bahnemann, Helv. Chim. Acta 84 (2001) 3742–3759.
[29] J. Feng, X. Hu, P.L. Yue, Ind. Eng. Chem. Res. 42 (2003) 2058–2066.